# Origin of Transconductance roll-off in mmWave AlGaN/GaN HEMTs

Terirama Thingujam[1], Michael J Uren[1], Niklas Rorsman[2], Matthew Smith[1], Andrew Barnes[3], Michele Brondi[4] and Martin Kuball[1]

[1]Center for Device Thermography and Reliability, H.H. Wills Physics Laboratory, University of Bristol, Tyndall Avenue, Bristol BS8 1TL, UK
[2]Department of Microtechnology and Nanoscience, Chalmers University of Technology, 412 96 Gothenburg, Sweden
[3] European Space Agency (ESA), Oxfordshire OX11 0FD. United Kingdom.
[4] Akkodis for European Space Agency (ESA), 2200 AG Noordwijk, The Netherlands
*Email: teri.thingujam@bristol.ac.uk, Phone: +44 117 331 8110

**Keywords: AlGaN/GaN, Linearity, LO phonon scattering, mmWave, Source starvation**

**Abstract**

**Transconductance roll-off at high gate bias is an issue in mmWave AlGaN/GaN HEMTs, resulting in reduction of current gain cut-off frequency, $f_T$ and degradation in linearity. In this work, the cause of this effect is investigated by comparing competing source starvation and hot phonon scattering models in TCAD simulations. Simulation of a GaN HEMT with a 100 nm gate length and recessed contact suggests that the device characteristics could be better explained by the source starvation model. This work highlights the importance of including source starvation effects in the design of device and optimization of RF device characteristics.**

## INTRODUCTION

AlGaN/GaN high electron field mobility transistors (HEMTs) exhibit excellent performance in high frequency applications. To further improve high frequency performance e.g for operation at 30 GHz and above, devices have been scaled down and novel technologies like graded channel have been implemented [1-3]. AlGaN/GaN HEMTs exhibit a gradual decrease in transconductance (roll-off) and cut-off frequency in on-state at high frequencies, thereby limiting linearity. Inability to maintain high transconductance for wider range of gate bias has been explained to be due to lower saturation velocity, $v_{sat}$ of GaN, than theoretically predicted [4, 5].

The underperforming saturation is often explained by two alternative ways, which has been under active research and debated. They are the saturation velocity limitation by hot phonon scattering at high carrier density [6, 7], and due to an increase in source resistance, $R_S$, with current (which is an example of a so-called source starvation) [5, 8, 9]. In this work, we implemented a source starvation model in TCAD and compared the result with the hot phonon scattering model, which is also known as longitudinal optical (LO) phonon model [10]. The simulations were compared to experimental DC and small signal RF data. The results impact design rules of high frequency GaN devices, and ultimately their manufacture.

## DEVICE STRUCTURE AND MODELS

Figure 1 shows the schematic structure of the simulated device under investigation. The AlGaN/GaN HEMT structure has T-gate with a footprint, $L_G$ of 100 nm, $Al_{0.3}Ga_{0.7}N$ barrier layer of 10 nm, 100 nm thick GaN channel, 300 nm thick Fe-doped GaN buffer and an AlN nucleation layer on a SiC substrate. The structural specifications of the AlGaN/GaN HEMT device under investigation is shown in Table I. The ohmic contacts were implemented via recessing and evaporation of a Ta/Al/Ta metal-stack, resulting in a sidewall contact to the 2DEG [11].

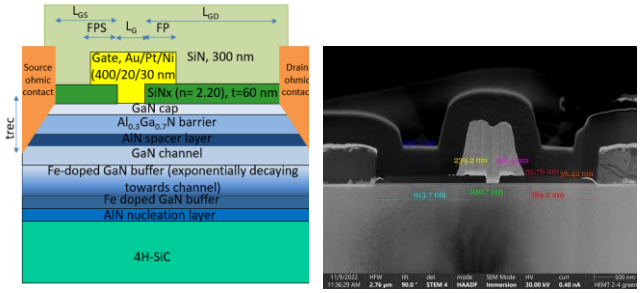


Fig. 1. (a) Schematics of the AlGaN/GaN device under investigation (b) STEM image of the fabricated device.

TABLE I

STRUCTURAL SPECIFICATIONS OF THE ALGAN/GAN DEVICE UNDER INVESTIGATION

| Layout Parameters | Value |
|---|---|
| $L_G$ | 0.1 µm |
| $L_{GD}$ | 1 µm |
| $L_{GS}$ | 0.65 µm |
| FPs | 0.15 µm |
| $t_{rec}$ | 23 nm |

A 2D physics-based simulation was carried out using Silvaco ATLAS. A 2DEG density of $9.2\times10^{12}$ $cm^{-2}$ was obtained from TCAD, which matches closely the Hall measured 2DEG of $1.05\times10^{12}$ $cm^{-2}$. The threshold voltage was calibrated to the measured result by proper surface pinning of the Fermi level, ~ 1eV below the conduction band, in the access region and setting the work function of the gate metal to 4.1 eV. A contact resistance $R_C$ of 0.272 ohm.mm is implemented, calibrated against 0.3 ohm.mm of the real device, measured from the TLM structure. To obtain a good fit to the $I_D$-$V_{DS}$ and $I_D$-$V_{GS}$ characteristics, two different approaches based on adjusting saturated velocity were implemented and compared.

Firstly, hot phonon scattering was implemented using the LO phonon model, which has been widely used, to explain the reduction of electron velocity in GaN at high carrier densities, as discussed in the previous section. The LO phonon model was contrasted with an alternative, a novel source starvation model, developed in this work to mimic the effect of a localized reduction in the carrier density near the ohmic contact. This creates a current-dependent source resistance, resulting from velocity saturation occurring at lower gate voltage than in the main part of the channel. This can happen for instance if there is localized strain relaxation associated with the etching and contact metallization and annealing. However, there are very few articles that explain source starvation effects and this work gives an observation on its impact.

## RESULTS AND DISCUSSION

The measured device exhibits a maximum current density of 1 A/mm, $g_m$=430 mS/mm. As a benchmark, Fig. 2 shows the comparison of simulation using a traditional carrier density independent $v_{sat}$ model ($v_{sat}$= 1.6 ×$10^7$ cm/s), compared with the measured data. It is found that current is two times higher than the measured one, also a greatly broader $g_m$ peak is observed in the TCAD model, confirming the necessity for a more sophisticated approach. The discrepancy can be seen most importantly in the transconductance curves (Fig 2 b), where simulated result gives a much broader, bell-shaped curve, while measured result shows a faster roll-off.

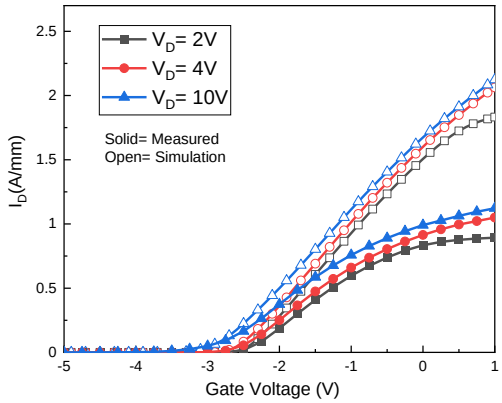


(a)

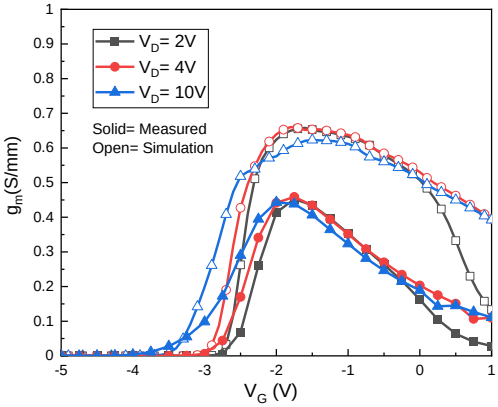


(b)

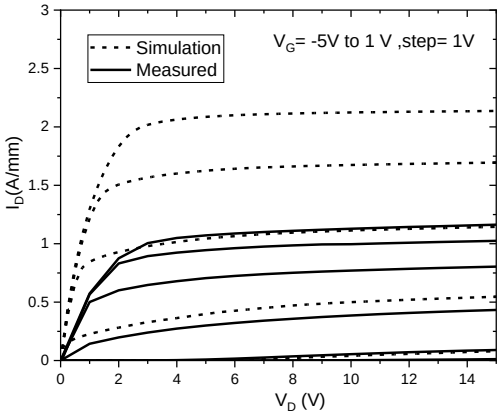


(c)

Fig 2. Comparison of the DC device performance from TCAD model, simulated with the regular $v_{sat}$ model, to measured data (a) $I_D$-$V_G$ characteristic (b) $g_m$-$V_G$ characteristic (c) $I_D$-$V_D$ characteristics.

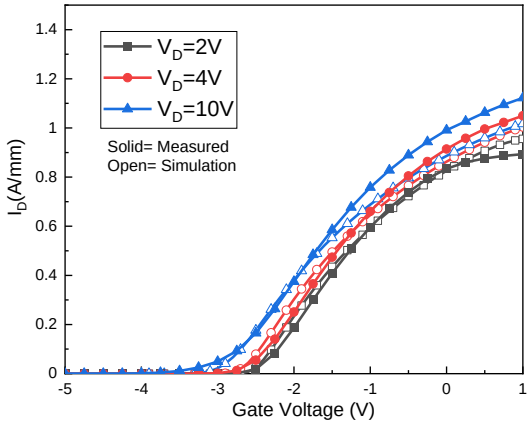


(a)

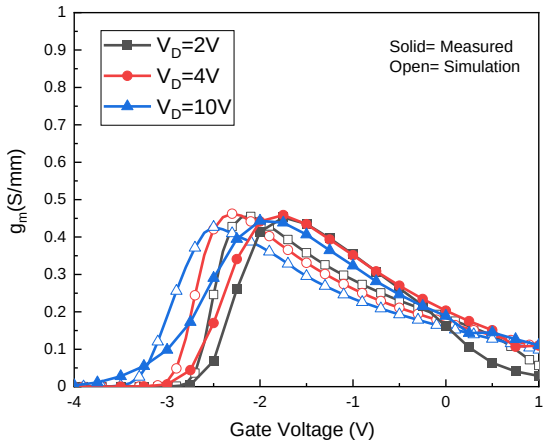


(b)

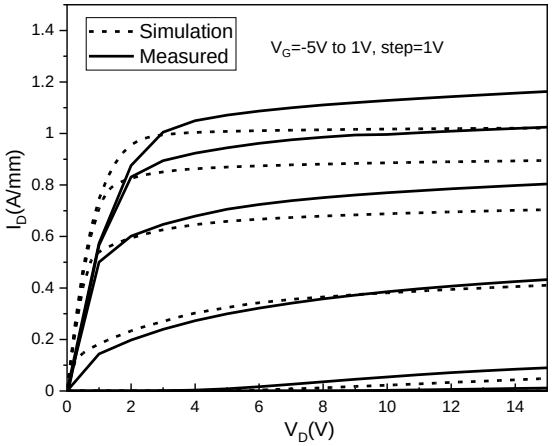


(c)

Fig 3. Comparison of the DC device performance from TCAD model, simulated with the LO phonon Model, to measured data (a) $I_D$-$V_G$ characteristic (b) $g_m$-$V_G$ characteristic (c) $I_D$-$V_D$ characteristics.

TABLE II

PARAMETERS USED IN THE LO PHONON MODEL IN THE REFERENCE VS OUR MODEL

| Parameters | Referred Model [4] | Our Model |
|---|---|---|
| Carrier density, $n_0$ (/cm$^3$) | $6\times10^{19}$ | $1.5\times10^{20}$ |
| Electron mobility, mu0 (cm/V. s) | 1320 | 1200 |

Fig 3 shows the device characteristics, simulated, and fitted with LO phonon model. A C-interpreter model, as employed in [4] was implemented, parameters used in this work are adjusted from the reference model (TABLE II) to improve fit to the experimental data. As seen, the decrease of $v_{sat}$ with carrier density due to the hot phonon scattering, implemented in this model, causes a rapid decrease of the simulated $g_m$ curve at high $V_{GS}$; this greatly improves the fit to the measured data. However, we can still notice a slightly faster roll-off in the transconductance, in the TCAD result some discrepancy is also apparent in the knee region (Fig 3 (c)).

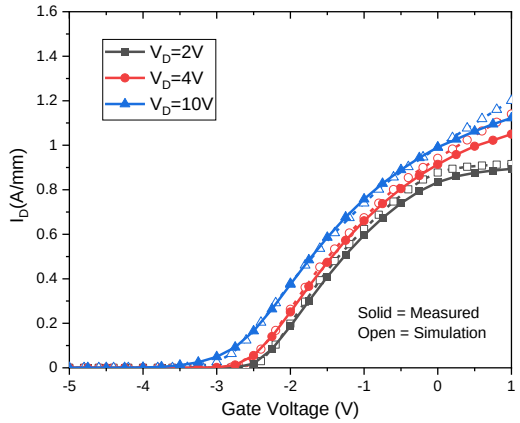


(a)

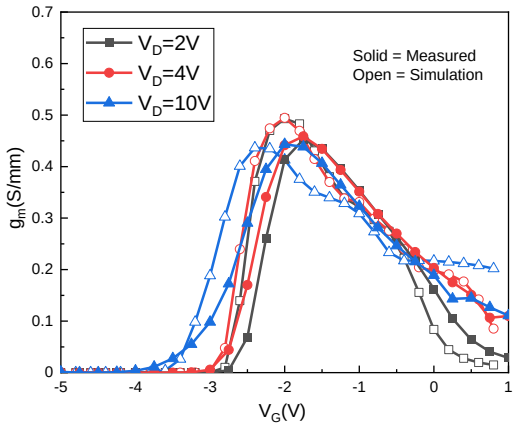


(b)

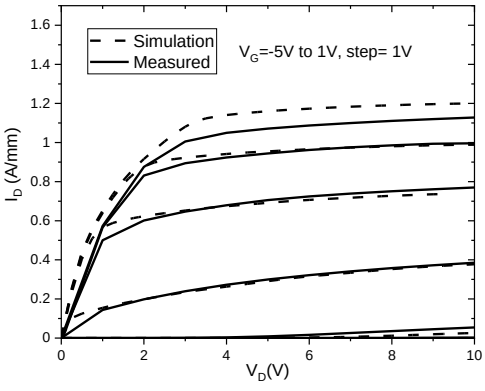


(c)

Fig 4. Comparison of the DC device performance from TCAD model, simulated with our source starvation model, to measured data (a) $I_D$-$V_G$ characteristic (b) $g_m$-$V_G$ characteristic (c) $I_D$-$V_D$ characteristics.

Fig. 4 shows TCAD result, simulated with the source starvation model, which is implemented by introducing a local lower carrier density near the source/drain contacts. In

contrast to the LO phonon model a general overall better fit to the experimental data is achieved. As seen in the $g_m$-$V_G$ curve in Fig. 4 (b), a decrease of $g_m$ can be seen, which matches the experimental data. This suggests that source starvation cannot be ignored in the device considered here.
Small signal simulation shows similar peak intrinsic cut-off frequency for the two models, with 70 GHz for LO phonon model and 74 GHz for the source starvation model. However, there is a clear difference in the $V_{GS}$ dependence as shown in Fig. 5. The source starvation model explains the measured $f_T$ dependence on $V_{GS}$ better than the LO phonon model, in which $f_T$ degrades rather more rapidly. The LO phonon model clearly is important to consider in device simulations as it reflects the actual decrease in mobility with carrier density, however in itself, it cannot explain the device characteristics in full. Source starvation is important to be included which will impact device design rules and cannot be neglected at least for the device studied here.

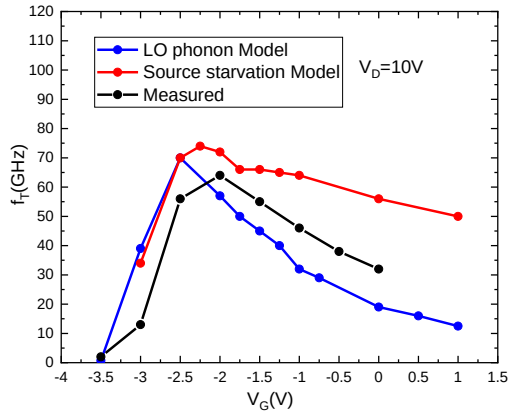


Fig. 5. Current gain vs $V_G$ simulated at $V_D$ = 10 V with different models, compared to the measured $f_{T,int}$

## Conclusions

LO phonon model and source starvation model were used to explain the gradual decrease of $g_m$ and $f_T$ at high $V_{GS}$, which degrades the linearity of millimeter-wave AlGaN/GaN HEMT devices. It was shown that simulation with the source starvation model can explain the device under investigation, better than the LO phonon model. While the LO phonon model is widely used to explain $g_m$ dependance of such devices, it is shown that the source starvation model can also explain this effect and indeed provides an improved fit to the reference device. It is likely that both effects can be present in short-gate length HEMTs, and both need to be considered in modelling of such devices.

## Acknowledgements

We acknowledge financial support from the European Space Agency under contract. 4000135857/21/NL/GLC/my in the frame of the Technology Development Element program (TDE). We also acknowledge Nikolai Drozdovski from the Materials & Electrical Components Laboratory of the European Space Agency for the results of the Focus Ion Beam Investigation.

## References

[1] P. Fay et. al, *Applied Physics Letters*, vol. 121, no. 14, p. 140502, 2022.
[2] J.-S. Moon *et al.*, *IEEE Electron Device Letters*, vol. 42, no. 6, pp. 796-799, 2021.
[3] J.-S. Moon *et al.*, *IEEE Electron Device Letters*, vol. 41, no. 8, pp. 1173-1176, 2020.
[4] P. S. Park, Doctor of Philosophy, Electrical and Computer Science, The Ohio State University, 2013.
[5] T. Palacios *et al.*, *IEEE Transactions on Electron Devices*, vol. 52, no. 10, pp. 2117-2123, 2005.
[6] S. Bajaj *et al.*, *IEEE Transactions on Electron Devices*, vol. 64, no. 8, pp. 3114-3119, 2017.
[7] J. B. Khurgin et al, *Applied Physics Letters*, vol. 107, no. 26, p. 262101, 2015.
[8] R. J. Trew et al, *IEEE Transactions on Microwave Theory and Techniques*, vol. 54, no. 5, pp. 2061-2067, 2006.
[9] K. Shinohara *et al.*, in *2012 International Electron Devices Meeting*, 2012: IEEE, pp. 27.2. 1-27.2. 4.
[10] N. Venkatesan et al, in *2019 IEEE BiCMOS and Compound semiconductor Integrated Circuits and Technology Symposium (BCICTS)*, 2019: IEEE, pp. 1-4.
[11] Y.-K. Lin *et al.*, *Semiconductor Science and Technology*, vol. 33, no. 9, p. 095019, 2018.

## Acronyms

LO: Longitudinal-optical
MBE: Molecular Beam Epitaxy
MOCVD: Metal Organic Chemical Vapor Deposition
TCAD: Technology Computer Aided Design